Pedosphere **34**(4): 749–758, 2024
doi: 10.1016/j.pedsph.2023.06.006
ISSN 1002-0160/CN 32-1315/P

Published by Elsevier B.V. and Science Press

PEDOSPHERE

www.elsevier.com/locate/pedosphere

^{15}N tracers and microbial analyses reveal *in situ* N_2O sources in contrasting water regimes of a drained peatland forest

Mohit MASTA[1], Mikk ESPENBERG[1,*], Laura KUUSEMETS[1], Jaan PÄRN[1], Sandeep THAYAMKOTTU[1], Holar SEPP[1], Kalle KIRSIMÄE[1], Fotis SGOURIDIS[2], Kuno KASAK[1], Kaido SOOSAAR[1] and Ülo MANDER[1]

[1]*Institute of Ecology and Earth Sciences, University of Tartu, Vanemuise Street 46, Tartu 51003 (Estonia)*
[2]*School of Geographical Sciences, University of Bristol, University Road, Bristol BS8 1SS (UK)*

(Received March 31, 2023; revised April 22, 2023; accepted May 11, 2023)

ABSTRACT

Managed peatlands are a significant source of nitrous oxide (N_2O), a powerful greenhouse gas and stratospheric ozone depleter. Due to the complexity and diversity of microbial N_2O processes, different methods such as tracer, isotopomer, and microbiological technologies are required to understand these processes. The combined application of different methods helps to precisely estimate these processes, which is crucial for the future management of drained peatlands, and to mitigate soil degradation and negative atmospheric impact. In this study, we investigated N_2O sources by combining tracer, isotopomer, and microbial analysis in a drained peatland forest under flooded and drained treatments. On average, the nitrification genes showed higher abundances in the drained treatment, and the denitrification genes showed higher abundances in the flooded treatment. This is consistent with the underlying chemistry, as nitrification requires oxygen while denitrification is anaerobic. We observed significant differences in labelled N_2O fluxes between the drained and flooded treatments. The emissions of N_2O from the flooded treatment were nearly negligible, whereas the N_2O evolved from the nitrogen-15 (^{15}N)-labelled ammonium ($^{15}NH_4^+$) in the drained treatment peaked at 147 μg ^{15}N m^{-2} h^{-1}. This initially suggested nitrification as the driving mechanism behind N_2O fluxes in drained peatlands, but based on the genetic data, isotopic analysis, and N_2O mass enrichment, we conclude that hybrid N_2O formation involving ammonia oxidation was the main source of N_2O emissions in the drained treatment. Based on the ^{15}N-labelled nitrate ($^{15}NO_3^-$) tracer addition and gene copy numbers, the low N_2O emissions in the flooded treatment came possibly from complete denitrification producing inert dinitrogen. At atomic level, we observed selective enrichment of mass 45 of N_2O molecule under $^{15}NH_4^+$ amendment in the drained treatment and enrichment of both masses 45 and 46 under $^{15}NO_3^-$ amendment in the flooded treatment. The selective enrichment of mass 45 in the drained treatment indicated the presence of hybrid N_2O formation, which was also supported by the high abundances of archaeal genes.

Key Words: denitrification, nitrification, N_2O, quantitative polymerase chain reaction

Citation: Masta M, Espenberg M, Kuusemets L, Pärn J, Thayamkottu S, Sepp H, Kirsimäe K, Sgouridis F, Kasak K, Soosaar K, Mander Ü. 2024. ^{15}N tracers and microbial analyses reveal *in situ* N_2O sources in contrasting water regimes of a drained peatland forest. *Pedosphere*. **34**(4): 749–758.

INTRODUCTION

Globally, peatlands cover a small part of land area, but they store about one-tenth of the global soil nitrogen (N) and can be a significant source of nitrous oxide (N_2O), which is a major greenhouse gas (Liu *et al*., 2020) and has a global warming potential 298 times higher than carbon dioxide. The current atmospheric N_2O level is the highest reported in the last 800 000 years and increasing (Hyodo *et al*., 2019; IPCC, 2021). In addition, N_2O is an important ozone depleter in the stratosphere (Ravishankara *et al*., 2019). Production of N_2O in soil is mainly associated with nitrification and denitrification. On the one hand, the nitrification process under aerobic conditions begins with the oxidation of ammonia to nitrite (NO_2^-) by ammonia monooxygenase *via* hydroxylamine, where the side product can be N_2O. On the other hand, denitrification happens under anoxic conditions, reducing nitrate (NO_3^-) and possibly producing N_2O if the process is not complete and N_2O is not transformed into dinitrogen (N_2) (Zhu *et al*., 2013; Hu *et al*., 2015).

The emissions of N_2O are controlled by many factors such as soil moisture, soil NO_3^- content, and temperature (Pärn *et al*., 2018; Masta *et al*., 2020). It has also been reported that N_2O emissions can follow a bell-shaped distribution against soil moisture, indicating high N_2O flux in the intermediate oxygen level range (Pärn *et al*., 2018; Masta *et al*., 2020). Even though there is knowledge about N_2O production mechanisms, it is still challenging to connect N_2O emissions to specific processes under certain conditions. This is because of the complex nature of microbial processes responsible for N_2O production, which could be active simultaneously (Kuypers *et al*., 2018).

Methods of measurement of N_2O from different microbial processes are limited. The ^{15}N tracer gas flux method is a

*Corresponding author. E-mail: mikk.espenberg@ut.ee.

common technique to partition sources, NO_3^- or ammonium (NH_4^+), of N_2O fluxes (Kulkarni *et al*., 2014; Sgouridis and Ullah, 2015, Kemmann *et al*., 2021). The ^{15}N-labelled tracer is injected into the soil, and the headspace is enclosed to ensure gas tightness. This ensures the headspace is enriched with $^{15}N_2O$, which can be measured to calculate the source of the emitted gas. One limitation of the method is that it can only be used to partition sources of N_2O (NO_3^- or NH_4^+) and not for the identification of processes. The method creates artificial conditions by adding ^{15}N, and hence isotope mapping cannot be used as it is based on natural abundances (Yu *et al*., 2020). In our study, we used tracer enrichment to identify the source of N_2O and not for partitioning processes (Stevens and Laughlin, 1998; Sgouridis and Ullah, 2015).

The isotopomers of N_2O, which differ by the central (α-) or terminal (β-) position of the heavy isotope in the N_2O molecule, have also been studied to connect N_2O to its origin in a specific process (Yu *et al*., 2020). The difference in ^{15}N natural abundance between the central and terminal positions of ^{15}N is called site preference of ^{15}N ($\delta^{15}N^{SP}$). It has been considered an indicator of the N_2O formation process (Toyoda *et al*., 2002). Production of N_2O in both nitrification and denitrification can cause enrichment of ^{15}N at both (α and β) positions of the N_2O molecule. Therefore, wide ranges of site preference have been reported for nitrification and denitrification processes. Even though nitrification and denitrification can be separated somewhat clearly using isotope mapping, some processes overlap, making it hard to point towards a specific process (Bol *et al*., 2003; Sutka *et al*., 2003, 2006, 2008; Well and Flessa, 2009; Hu *et al*., 2015). In symmetric intermediates, such as hyponitrite ($^-ONNO^-$), cleavage of the ^{15}N–^{16}O bond is likely the reason for differences in $\delta^{15}N^{SP}$ values (Schmidt *et al*., 2004; Baggs, 2008). On one hand, $\delta^{15}N^{SP}$ values can be used to identify the processes behind N_2O fluxes, as we did in our study. On the other hand, the method poses an inherent problem of overlapping $\delta^{15}N^{SP}$ ranges. Hence, microbial data should back up the isotopomer mapping to get a clear understanding of N_2O production and consumption processes.

For microbial analysis, quantitative polymerase chain reaction (qPCR) offers a precise, sensitive, and fast real-time method to measure the relative shares of genes responsible for different processes in the N cycle (Smith *et al*., 2006; Smith and Osborn, 2009; Levy-Booth *et al*., 2014). It should be noted that qPCR shows the potential for processes, but only N_2O fluxes (in relationship with gene abundance) show gene activity. Disadvantages of the method include possible bias in PCR amplification and poor primers coverage. Bacterial and archaeal *amoA* are the key genes responsible for nitrification. For denitrification, *nirK* and *nirS* are the key controlling genes, along with *nosZI* and *nosZII* responsible for the final step of denitrification (reduction of N_2O to N_2) (Kuypers *et al*., 2018). Furthermore, the still recently overlooked group of microbes possessing the *nosZII* gene includes a significant fraction of non-denitrifying N_2O reducers, which could be solely a sink for N_2O (Hallin *et al*., 2018). All in all, a combined study of key functional genes and isotopic analysis of N_2O can further explain N_2O production and consumption pathways.

Studies on ^{15}N tracer and N cycle control genes have been integrated with a limited number of studies. Ma *et al*. (2008) used such a combined approach to analyze the relationship between nitrifier and denitrifier community composition and abundance in predicting N_2O emissions from pothole peat soils. Suenaga *et al*. (2021) used the combination of ^{15}N tracer and microbial analyses to disclose the N_2O sink potential of the anammox community. In their review papers, Hu *et al*. (2015) and Yu *et al*. (2020) also mentioned the importance of a combined approach. Nevertheless, the full range of N cycle control genes has not been used in previous studies.

Our study aimed to identify, quantify, and compare processes responsible for N_2O emissions in a drained peatland forest by analyzing relationships of gene abundances and isotopic signatures from ambient N sources and ^{15}N-labelled tracers (NO_3^- and NH_4^+) under the drained and flooded water regimes. We hypothesised that: i) higher N_2O emissions occur in the drained soil as compared to the flooded, ii) based on the labelled ^{15}N, NH_4^+ is the dominant source of N_2O in the drained treatment, whereas NO_3^- dominates as the source of N_2O under the flooded conditions, and iii) bacterial, archaeal, and comammox nitrification and nitrifier denitrification are the dominant processes of N_2O emissions under the drained treatment, whereas incomplete and complete denitrification are responsible for N_2O fluxes under the flooded treatment.

MATERIALS AND METHODS

Study site

A drained peatland near the settlement of Agali (58°17′ N, 27°19′ E) in the Järvselja Experimental Forest District, Kastre Municipality, Southeast Estonia was the experimental site (Fig. S1, see Supplementary Material for Fig. S1). The experimental site was in a mixed forest mainly dominated by spruce and birch trees. The site is close to the Apna Ditch. In July 2020, three equilateral triangles (1.6 m in side) were constructed for each soil moisture regime (flooded and drained) (Fig. S1). Wooden planks were used to make the sides of these triangles, and each side had a depth of 40 cm and a height (above soil surface) of 20 cm. One water table observation well was also installed in each triangle. Flooding/draining wells were installed at the center of each triangle, and three circular collars with a diameter of 65 cm

were installed for gas measurements at a depth of 10 cm from the soil surface. The drained and flooded triangles were about 10 m apart, and they began in October 2020 and finished in January 2021. The water for flooding was extracted from the Apna Ditch. In the drained triangles, water was drained *via* central wells using a pump. Flooding began after pre-treatment sampling and continued for the rest of the experiment. Anoxic conditions were achieved during the short-term flooding in the flooded treatment, and the water table was raised to 20 cm above the soil surface. Flooding was stopped one hour before each sampling session to apply the tracer. The soil moistures for drained triangles were in the range of 50%–65%, and for flooded were 71%–92%.

Soil chemical characteristics are shown in Table SI (see Supplementary Material for Table SI). The soil had high organic matter content, showing rich material for peat formation, and the pH was slightly acidic. Overall, the soil properties were similar between the drained and flooded triangles before tracer amendment.

Gas and soil sampling

Gas and soil sampling took place six times between October 6, 2020 and January 7, 2021. Samples were collected during two separate NO_3^- (October 20, 2020 and November 26, 2020) and NH_4^+ (October 27, 2020 and November 30, 2020) amendment sessions. One pre- (October 6, 2020) and one post-amendment (January 7, 2021) sessions were conducted as control observations. We aimed for a 5% enrichment of the respective NO_3^- and NH_4^+ contents in the soil. To achieve that, Sigma Aldrich (USA) 98 atom% $K^{15}NO_3$ and $^{15}NH_4Cl$ tracers were prepared. Each tracer was mixed with water taken from the nearby ditch to make a tracer solution of 250 mL. Each session lasted for an hour and started 15 min after the injection of the tracer into the top 5 cm of the soil inside a collar. Polyvinyl chloride chambers (65 L) were installed on top of collars (Soosaar *et al*., 2011) inside the triangles, and pre-vacuumed glass vials were used to collect gas samples. Gas samples were collected at the beginning of each session, followed by sampling after every 20 min for an hour. Glass vials (50 mL) were used to collect gas samples for the calculation of N_2O emissions, and 100-mL vials were used for gas isotope analysis. The gas isotope samples were collected at the end of each session, with three samples per session.

Soil samples (nine for each analysis from both treatments) were collected for soil physiochemical, isotope, and microbiological analyses in separate plastic bags on all sampling days. We collected 108 soil samples in total for each analysis. The soil was collected from each collar of each triangle at a depth of 10 cm. Until the chemical analyses, the soil samples were stored at 4 °C in a refrigerator. Until the microbiological analysis, the samples were stored in a −20 °C freezer.

Soil physicochemical analyses

Soil samples were collected from the top 10 cm from all six triangles for all treatments on all sampling days. Soil pH, NH_4^+, NO_3^-, total N, total phosphorus (P), total potassium, total calcium, total magnesium, and organic matter were measured according to the standard methods (APHA-AWWA-WEF, 2005). Soil temperature was also measured on all sampling days at depth of 10 cm.

Soil microbiological analysis

Soil total DNA was isolated using a DNeasy Powersoil Pro kit (Qiagen, Germany), and the protocol provided by the manufacturer was followed. Briefly, DNA was isolated from 0.25 g of wet soil sample, and a Precellys 24 machine (Bertin Technologies, France) was used to homogenize the samples at 5 000 r min^{-1} for 20 s. An infinite 200 M spectrophotometer (Tecan AG, Switzerland) was used to assess DNA quality and concentration. The isolated DNA was kept at −20 °C for further analysis.

The reaction of qPCR was used to quantify the 16S rRNA genes of bacteria and archaea as well as the nitrification (bacterial and archaeal *amoA*) and denitrification (*nirK*, *nirS*, *nosZI* and *nosZII*) genes. A Rotor Gene Q thermocycler (Qiagen, Germany) was used to perform the qPCR reactions. The volume of the reaction mixture was 10 μL, and it contained forward and reverse primers, 5 μL Maxima SYBR Green Master mix reagent (Thermo Fisher Scientific, USA), and 1 μL isolated DNA (Table SII, see Supplementary Material for Table SII). Every sample was amplified in triplicate, and three DNA-free negative control samples were added to all qPCR measurements. The qPCR results were evaluated with Rotor-Gene® Q software v.2.0.2 (Qiagen, Germany) and LinRegPCR v.2020.2. Standard curve ranges were used to calculate the number of gene copies. The qPCR methodology is described in more detail by Espenberg *et al*. (2018).

N_2O gas and isotope analysis

The amount of N_2O emissions from soil was measured using a gas chromatograph (GC-2014, Shimadzu, Japan) equipped with a flame ionization detector and an electron capture detector and coupled with a Loftfield autosampler (Loftfield *et al*., 1997).

For source partitioning of N_2O emissions, 98 atom% $K^{15}NO_3$ and $^{15}NH_4Cl$ tracers (Sigma Aldrich, USA) were used to reach a 5% enrichment to the original NO_3^- and NH_4^+ pools (Kulkarni *et al*., 2014). Tracer solution (250 mL) was injected into the top 5 cm of each collar inside drained and flooded triangles using a 50-mL syringe five times into five zones (center, left, right, top, and bottom) every time, with *ca*. 10 mL into each zone to ensure even distribution. It should

be noted that the tracers were used to partition the source (NO_3^- or NH_4^+) of N_2O emissions and not for partitioning the processes. Fluxes of ^{15}N-N_2O were calculated according to Buchen *et al*. (2016). Initial R45/44 and R46/44 values were used to achieve oxygen correction according to Bergsma *et al*. (2001). Then, a fraction of N_2O emitted from the tracer pool was calculated, and this fraction was used to calculate the final ^{15}N-N_2O fluxes from the total N_2O fluxes (Buchen *et al*., 2016; Zaman *et al*., 2021).

The isotopic composition of N_2O was measured using a Delta V Advantage isotope ratio mass spectrometer (IRMS) (Thermo Fisher Scientific, USA) coupled with a modified online concentration system Precon and GasBench II (Masta *et al*., 2020). The IRMS was equipped with a Universal 3 collector and the amplifier resistor values for faraday cups were 3×10^8, 3×10^{10}, and 1×10^{11} for masses 44, 45, and 46, respectively. The amplifier resistor values for masses 30 and 31 were 3×10^8 and3×10^{11}, respectively. As three-cup calibration needed to be performed for the IRMS, it was not possible to measure all the masses (44, 45, 46, 30, and 31) at once. Hence, N_2O and NO were measured with two sequences as three vials (100 mL each) were sampled for isotope analysis during each session, with one vial for N_2O measurement and two for NO to ensure a good signal in the IRMS (Well *et al*., 2006). The gas isotope calculation based on Toyoda and Yoshida (1999) was used to calculate $\delta^{15}N^{SP}$ (‰) for each measurement as follows:

$$\delta^{15}N^{SP} = \delta^{15}N^{\alpha} - \delta^{15}N^{\beta} \quad (1)$$

where $\delta^{15}N^{\alpha}$ and $\delta^{15}N^{\beta}$ are the ^{15}N natural abundances of central (α) N and terminal (β) N of N_2O, respectively (‰). Medical N_2O from Linde Gas and N_2O produced *via* thermal decomposition of NH_4NO_3 were used as lab standards for the IRMS. These were then calibrated according to Thünen Institute's standards (Well *et al*., 2006; Well and Flessa, 2009), which were calibrated according to the Tokyo Institute of Technology standards (Toyoda and Yoshida, 1999). Site preference values from tracer amendment sessions could be compared with the controls because the added ^{15}N tracer artificially changed the natural isotopic abundances. Site preference values were only calculated for pre- and post-experiment sessions where no tracer was added. Site preference values were used to partition the respective processes responsible for N_2O production and consumption.

Statistical analysis

STATISTICA v.7.1 was used for the *t*-test to determine the differences in NH_4^+ and NO_3^- contents and gene copy numbers. Spearman correlations were determined between the soil physicochemical parameters and gene copy numbers. Linear regression was used to compare the enrichment of R45/44 *vs*. R46/44 under different amendments. Interpolated contour plots were created using the akima package version 0.6-2.3 (Akima *et al*., 2021). The gene parameters were used as dimension z, and $\delta^{15}N^{SP}$ and $\delta^{18}O$ were used as the x and y axes, respectively. R version 4.1.2 was used to explore, harmonize, analyze, and visualize the data.

RESULTS AND DISCUSSION

Soil NO_3^--N and NH_4^+-N and their relationships with N_2O

Our results showed that soil NO_3^--N contents in the drained and flooded treatments were in the same range before the amendment sessions. After the first amendment, NO_3^--N was higher and increased only in the drained treatment, whereas it dropped and remained lower in the flooding treatment throughout the whole experiment (Fig. 1). The

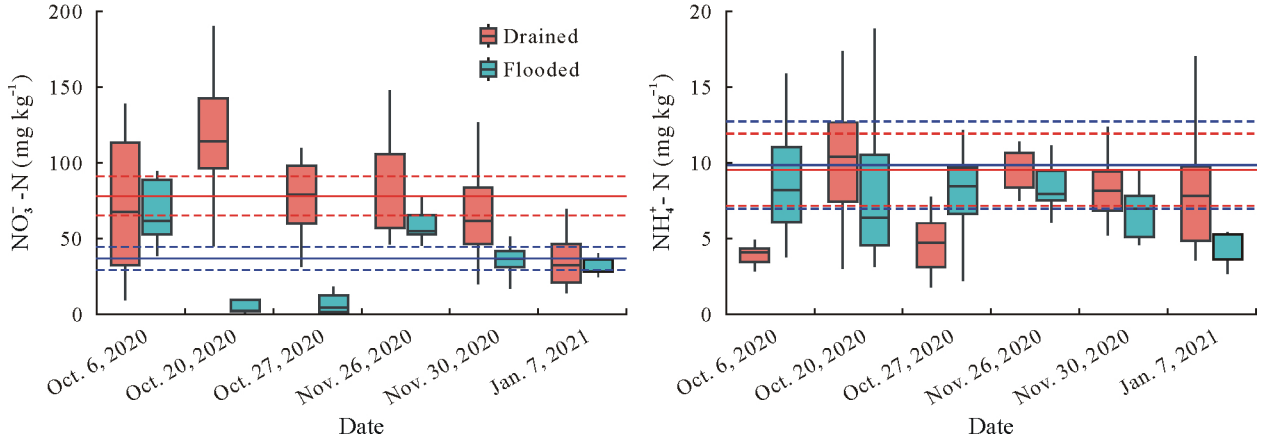

Fig. 1 Soil NO_3^--N and NH_4^+-N contents throughout the experiment in the drained and flooded treatments of a drained peatland forest near the settlement of Agali in the Järvselja Experimental Forest District, Kastre Municipality, Southeast Estonia. Tracer solution $K^{15}NO_3$ was injected into the top 5 cm of soil on Oct. 20 and Nov. 26, 2020, and tracer solution $^{15}NH_4Cl$ was injected on Oct. 27 and Nov. 30, 2020. Central lines within boxes indicate median values, box edges indicate the 25th and 75th percentiles, and whiskers represent the 95% confidence interval. The overall means and 95% confidence intervals are shown by the solid and dashed lines, respectively.

NO_3^--N content in the drained treatment declined continuously after the first amendment to the same level as that in the flooded site by the post-amendment session. In contrast, soil NH_4^+-N was initially low in both treatments before the first amendment and did not show any major difference between the two treatments throughout the experiment.

The N_2O emissions were higher from the drained treatments by orders of magnitude and generally higher under high soil NO_3^- and NH_4^+ contents (Fig. 2). In the flooded treatment, soil NO_3^- and N_2O flux levels were lower. The N_2O emissions were 368.0 ± 574.2 and 1 044.5 ± 1 654.8 μg N m^{-2} h^{-1} for drained treatment under NO_3^- and NH_4^+ amendments, respectively. For the flooded treatment under NO_3^- and NH_4^+ amendments, N_2O emissions were 2.9 ± 3.9 and 39.1 ± 42.3 μg N m^{-2} h^{-1}, respectively.

The N_2O emissions increased with increasing soil NO_3^- content. Under the flooded treatment, NO_3^- and N_2O flux levels were lower than in the drained treatment, possibly indicating the presence of complete denitrification. Under the drained treatment, NO_3^- levels were the highest with high N_2O fluxes. Increasing N_2O emissions with the increase in soil NO_3^- were also reported by Pärn *et al.* (2018) in their global study of N_2O emissions from organic soils. Similar relations of soil NO_3^- with N_2O emissions have been observed by Huang *et al.* (2014), who concluded that denitrification dominates N_2O emissions in acidic soils. In this study, the peat soil was similarly acidic, and hence, the soil NO_3^- is expected to play a major role in N_2O emissions. It is also possible that part of NO_3^- was formed *via* the oxidation of organic N, a pathway that has recently been considered and accounted for up to 83% of total NO_3^- production in laboratory experiments, especially in soils with lower P contents (O'Neill *et al.*, 2021). High organic matter and relatively low P content in the soil, important preferences for this pathway, are typical for our study area.

Source partitioning of N_2O emissions and isotope enrichment

There were significant differences in the evolution of $^{15}N_2O$ between the drained and flooded treatments (Fig. S2, see Supplementary Material for Fig. S2). The N_2O emissions from the flooded treatment were negligible, whereas the N_2O evolved from NH_4^+ in the drained treatment peaked at 147 μg ^{15}N m^{-2} h^{-1}. The N_2O emitted was enriched with ^{15}N under both $^{15}NO_3^-$ and $^{15}NH_4^+$ amendments (Fig. 3). Under the $^{15}NO_3^-$ amendment, N_2O was enriched with both masses 45 and 46, and the magnitude of mass 46 was higher than that of mass 45. Enrichment of mass 46 indicated enrichment of ^{15}N on both (α and β) positions of the N_2O molecule, considering that the abundance of ^{18}O was in natural conditions. For mass 45 (one ^{15}N atom in the N_2O molecule), our results showed the preference of ^{15}N for the α position. The $^{15}NH_4^+$ amendment showed enrichment in N_2O largely with mass 45, indicating enrichment in one position

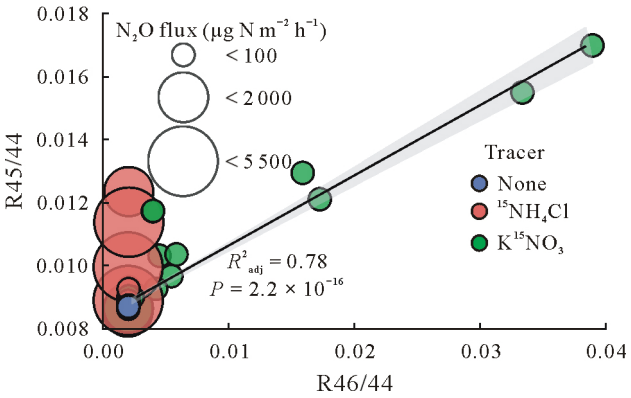

Fig. 3 Relationship between N_2O molecular mass ratios R45/44 and R46/44 with injections of different tracer solutions ($^{15}NH_4Cl$ and $K^{15}NO_3$) into the soil along with total N_2O flux in the drained treatment of the experiment conducted on a drained peatland forest near the settlement of Agali in the Järvselja Experimental Forest District, Kastre Municipality, Southeast Estonia. The shaded area on both sides of the regression line represents the 95% confidence interval. R^2_{adj} = adjusted R^2.

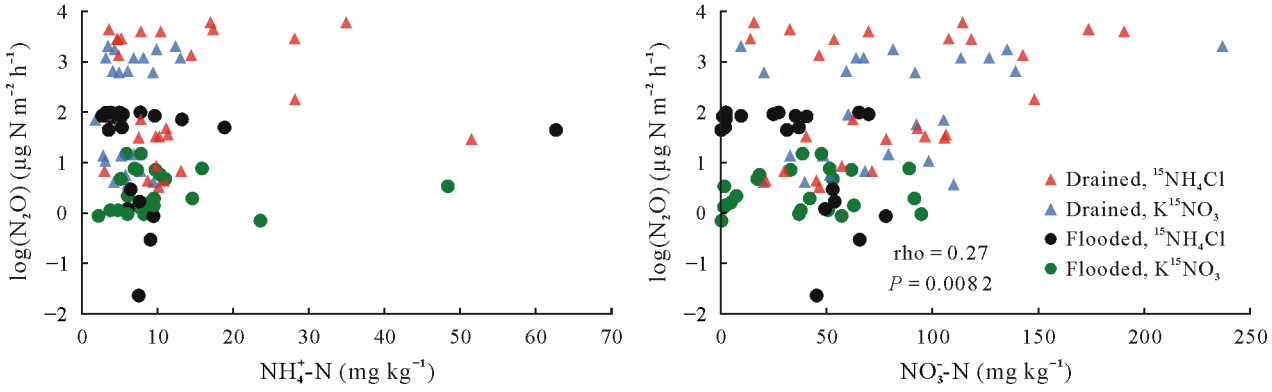

Fig. 2 Changes in N_2O emissions with soil NH_4^+-N and NO_3^--N contents in the drained and flooded treatments of a drained peatland forest near the settlement of Agali in the Järvselja Experimental Forest District, Kastre Municipality, Southeast Estonia. Tracer solutions $^{15}NH_4Cl$ and $K^{15}NO_3$ were injected into the top 5 cm of soil during the experiment. Spearman's rho and P values were used to check for correlation strength and significance between N_2O emissions and soil NH_4^+-N and NO_3^--N contents (rho and P values for non-significant relationship are not shown). log(N_2O) = logarithmic N_2O flux.

of the N_2O molecule. The enrichment of one position only may be due to hybrid processes of N_2O formation, where one N is coming from the tracer and another is coming from a co-substrate (N compound in soil). Normal nitrification where all the N originates from $^{15}NH_4^+$ must result in nearly equal ^{15}N enrichment of both positions. The positive $\delta^{15}N^{SP}$ values in the $^{15}NH_4^+$ amendment showed that the enrichment of ^{15}N took place at the α position. We also found that N_2O emissions were high under the NH_4^+ amendment and low for the NO_3^- amendment.

The ^{15}N tracer amendment resulted in the enrichment of mass 45 (^{14}N-^{15}N-^{16}O, ^{15}N-^{14}N-^{16}O, or ^{14}N-^{14}N-^{17}O) and 46 (^{15}N-^{15}N-^{16}O, ^{14}N-^{14}N-^{18}O, ^{14}N-^{15}N-^{17}O, or ^{15}N-^{14}N-^{17}O) of the N_2O molecule. The $^{15}NH_4^+$ amendment showed a selective enrichment of mass 45 of the N_2O molecule under drained treatment. On the other hand, NO_3^- amendment under flooded treatment resulted in the enrichment of masses 45 and 46 of the N_2O molecule, with a linear correlation between mass 45 and 46. It should be noted that during tracer labelling, it is possible to get an underestimation of enrichment due to inhomogeneity and hence it is better to check the enrichment using multiple methods of calculation (Arah, 1992; Deppe *et al*., 2017). The enrichment level of mass 46 was higher than mass 45, indicating that the tracer was the source of enrichment as under natural abundances, mass 45 dominates over mass 46 for N_2O. This could be another indicator of distinct processes under the drained and flooded treatments. It has been reported that N_2O formed during nitrification is more depleted in ^{15}N and ^{18}O than in denitrification. This explains why $^{15}NH_4^+$ was the precursor of N_2O under drained conditions, showing enrichment of mass 45 in N_2O (Yu *et al*., 2020). The selective enrichment of mass 45 under drained treatment and $^{15}NH_4^+$ amendment also indicates hybrid N_2O production. During this process, one N (α position) comes from the tracer ($^{15}NH_4^+$) injected and another one comes from the co-substrate (NO_2^-) under dominance of archaeal gene such as ammonia-oxidizing archaea (Stieglmeier *et al*., 2014). In our study, archaeal genes were dominant under drained treatment and hence hybrid N_2O production that involves ammonia oxidation might be a major source of the N_2O emissions. If nitrification was dominant under drained conditions in our study, we would also expect to detect mass 46 of the N_2O molecule, considering that we injected $^{15}NH_4^+$ as a tracer. Reduction of N_2O to N_2 causes the differences in $\delta^{15}N$ to occur while leaving the unreacted N_2O gas more enriched in ^{15}N (Schmidt *et al*., 2004; Baggs, 2008). The N_2O produced in our flooded peat showed enrichment of both heavy masses (45 and 46). This indicates that denitrification of $^{15}NO_3^-$ was the source process of the small amount of N_2O produced in our flooded treatment. This is also supported by N_2O emissions, which were low for the NO_3^- amendment and high for the NH_4^+ amendment. Hence, we observed hybrid N_2O formation and nitrification as the driving processes for N_2O emissions under drained treatment and the presence of complete denitrification under flooded treatment. In the case of tracer studies, it is not common to perform IRMS to get enrichment for calculation of $\delta^{15}N^{SP}$, as this is conducted with natural abundances. However, it should be noted that the tracer application amplifies the enrichment of each process and can provide insight into individual process identification. Even though the site preference values after tracer application cannot be used for process partitioning, we found that mass enrichment can still be used to get some insight into nitrification, denitrification, and hybrid N_2O processes.

Soil gene copies and their relations with environment characteristics

There was no clear difference in the bacterial gene copy numbers between the flooded and drained treatments during the amendment sessions (Fig. S3a, see Supplementary Material for Fig. S3). Archaeal 16S rRNA gene copy numbers were higher in the drained treatment (Fig. S3b). On average, bacteria showed higher abundances in the flooded sites, and archaea were more abundant in the drained sites.

Under the NH_4^+ amendment, the abundance of bacterial *amoA* was slightly higher under the drained treatment than under the flooded treatment, but there was not much overall difference (Fig. S4, see Supplementary Material for Fig. S4). In general, the abundances of archaeal *amoA* were higher under the drained treatment, although both treatments showed very similar abundances at the end of the experiment.

Under the $^{15}NO_3^-$ amendment, *nirS* gene copy numbers were higher under drained conditions compared to flooded conditions, although overall, they showed similar abundances (Fig. S5, see Supplementary Material for Fig. S5). However, a temporal trend was observed for both treatments as the abundances of *nirS* genes decreased with lower temperatures. The *nirK* gene copy numbers were lower in the drained treatment as compared to the flooded for both tracer ($^{15}NO_3^-$ and $^{15}NH_4^+$) amendments. Overall, *nosZI* gene copy numbers were higher in flooded conditions compared to drained. Like in *nirS* abundances, the two treatments were similar in gene copy numbers of *nosZII*. Fungal and bacterial denitrification were observed as dominant processes based on the isotopic mapping (Fig. 4).

Correlations between different soil physicochemical parameters and functional gene abundances are shown in Fig. S6 (see Supplementary Material for Fig. S6). Positive correlations were observed between soil NO_3^-, temperature, and the abundances of *nirK* and *nosZI* genes, but pH was negatively related to these gene abundances. The *nirS* gene abundances were negatively correlated with temperature and soil NO_3^-. The higher ratio of *amoA* nitrification and

nir denitrification genes indicates the greater abundance of *amoA* genes under drained treatment and also shows their significant contribution to N_2O (Fig. 5a). When we compared the N_2O consumers (*nosZ*) to producers (*nir* and *amoA*), we saw that the smallest emissions came from the flooded treatment where the *nosZ* abundances were high (Fig. 5b).

Bacteria were higher in the flooded treatment, but archaea were higher under the drained treatment. This might have been for the preference of archaeal genes towards quite dry peatlands, which was also observed by Espenberg *et al.* (2018). Under the $^{15}NH_4^+$ amendment, archaeal genes were higher in the drained treatment. Gene copies for archaeal *amoA* were higher in the drained treatment, suggesting archaeal nitrification under aerobic conditions (Barnard *et al.*, 2005). The denitrification gene *nirK* and *nosZI* copies were low under the drained treatment as denitrification is favored under anaerobic conditions (McKenney *et al.*, 2001). Under both water regimes, *nirS* dropped with decrease in soil temperature. This might be due to the higher temperature sensitivity of microbes with *nirS* genes as compared to those with *nirK* genes (Xing *et al.*, 2021). Hence, higher involvement of the *nirK* microbes in the production of N_2O can be expected under lower temperatures. The number of *nosZII* gene copies in the drained treatment and *nosZI* in the flooded treatment were negatively correlated with N_2O emissions. Such correlation has also been observed

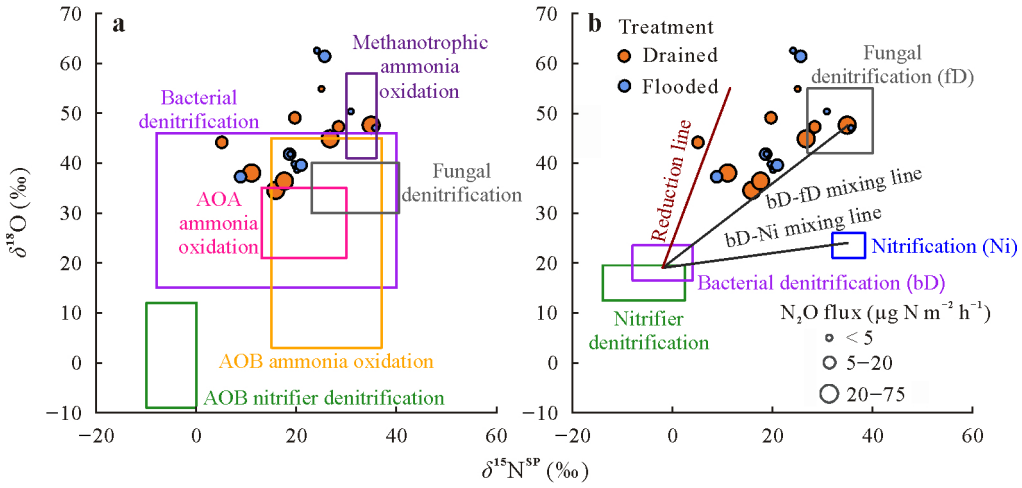

Fig. 4 Site preference of ^{15}N ($\delta^{15}N^{SP}$) (*i.e.*, ^{15}N natural abundance difference between the central N and terminal N of N_2O), ^{18}O natural abundance difference ($\delta^{18}O$), and N_2O emissions in the drained and flooded treatments that did not receive tracer in the experiment conducted on a drained peatland forest near the settlement of Agali in the Järvselja Experimental Forest District, Kastre Municipality, Southeast Estonia. The colored boxes indicate the expected ranges for microbial processes based on Hu *et al.* (2015) (a) and Yu *et al.* (2020) (b). AOA = ammonia-oxidizing archaea; AOB = ammonia-oxidizing bacteria.

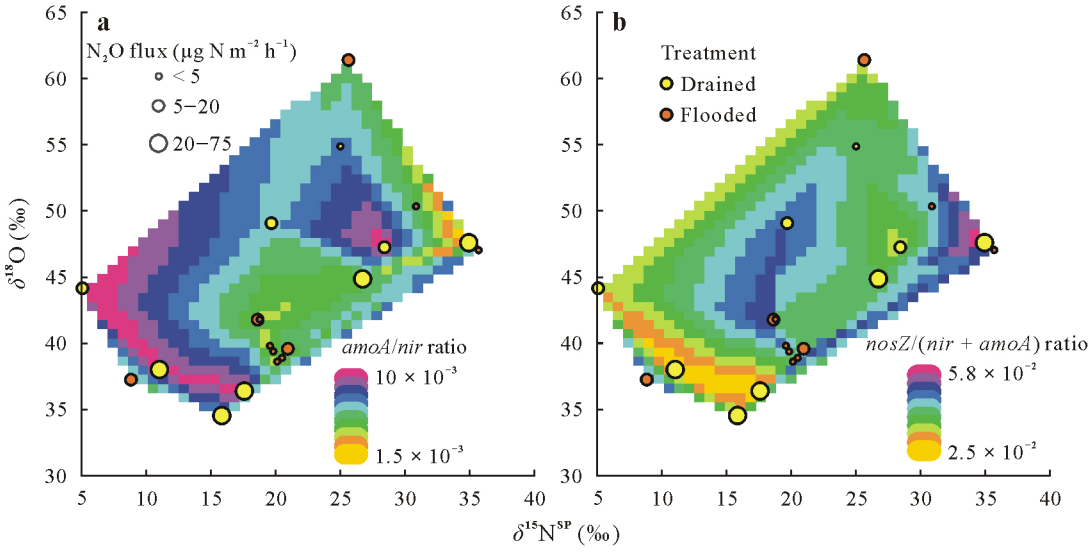

Fig. 5 Relationships between ^{15}N site preference ($\delta^{15}N^{SP}$) (*i.e.*, ^{15}N natural abundance difference between the central N and terminal N of N_2O) and ^{18}O natural abundance difference ($\delta^{18}O$), *amoA*/*nir* (a) and *nosZ*/(*nir* + *amoA*) (b) gene abundance ratios, and N_2O fluxes in the drained and flooded treatments of a drained peatland forest near the settlement of Agali in the Järvselja Experimental Forest District, Kastre Municipality, Southeast Estonia. The gene abundance ratios were plotted as the *z* dimension.

in a tropical peat bog of French Guiana (Espenberg *et al*., 2018). This shows different ecological niches of microbes with *nosZI* and *nosZII* genes (Jones *et al*., 2013). Under the drained treatment, *nosZII* was more likely to reduce N_2O, but under flooded treatment, *nosZI* was likely the N_2O-reducing gene.

N_2O isotopomers and combination with microbial methods

We fitted our $\delta^{15}N^{SP}$ and $\delta^{18}O$ values from the control sessions into the context of two previous studies (Hu *et al*., 2015; Yu *et al*., 2020) (Fig. 4) that separate processes based on those values. Our values varied in a narrow range of the reference plots and showed overlapping processes. The values of $\delta^{15}N^{SP}$ indicate the presence of bacterial denitrification, bacterial nitrification, and fungal denitrification (Hu *et al*., 2015; Yu *et al*., 2020). The gene parameters added information on the source processes (Fig. 5). We observed high N_2O emissions under the drained treatment, where *amoA* gene abundances were high as well. Similarly, under the flooded treatment, we observed low N_2O emissions with high *nos*Z gene abundances, indicating the reduction of N_2O under these conditions. On comparing nitrifier (*amoA*) and denitrifier (*nir*) genes regarding the production of N_2O, we found that the contribution of *amoA* genes was higher. Also, on comparing consumer (*nos*) and producer (*nir* + *amoA*) genes for N_2O, we found that in regions where consumer gene abundances were high, N_2O emissions were low and *vice versa* for producer gene abundances, which were responsible for high N_2O emissions. The site preference values indicate the presence of multiple processes overlapping each other, but with the combination of microbial and site preference values, we can make a more precise estimate regarding the processes responsible for N_2O production and consumption.

The high $^{15}N_2O$ flux evolved from $^{15}NH_4^+$ and indicated towards nitrification in the drained peat. In both the flooded and drained treatments, $\delta^{15}N^{SP}$ values increased with increasing $\delta^{18}O$ and were found to be positive. Positive site preference values have been reported for different processes before, such as ammonia oxidation (13‰ to 34‰), fungal denitrification (22‰ to 40‰), and bacterial denitrification (-7‰ to 24‰) (Well and Flessa, 2009; Hu *et al*., 2015; Yu *et al*., 2020). This clearly shows the problem of overlapping among different processes. Our $\delta^{15}N^{SP}$ data showed bacterial denitrification and bacterial nitrification as the driving processes according to the study of Hu *et al*. (2015), but based on Yu *et al*. (2020), our $\delta^{15}N^{SP}$ values lie on the boundary of fungal and bacterial denitrification. These isotope mapping models differ mainly in the presented $\delta^{15}N^{SP}$ values, and although Hu *et al*. (2015) include more processes, the ranges are large, and the effect of N_2O reduction is ignored. Yu *et al*. (2020) presented a much more precise summary of the $\delta^{15}N^{SP}$ values as they only considered $\delta^{15}N^{SP}$ values, which directly affect N_2O emission, and N_2O reduction was presented as a separate process. On the other hand, N_2O fluxes obtained from the ^{15}N gas flux method initially indicated nitrification as the major source, as the NH_4^+ tracer was the source of these emissions. Hence, for a more precise estimate of N_2O production and consumption processes, it is better to combine microbial and isotopic results. We recorded higher gene copy numbers for *amoA*, *nosZII*, and archaeal 16S rRNA under the drained treatment. We should also consider that the proportion of *nosZ* is lower than that of *amoA* in forest soils, which indicates the dominance of nitrification genes under drained conditions. Moreover, the results from isotope enrichment indicate presence of a hybrid N_2O formation process due to the selective enrichment of mass 45 of N_2O. If nitrification was the major source of N_2O emissions under the drained treatment, we should have also observed mass 46 in our results as the applied $^{15}NH_4^+$ must have oxidized to form $^{15}N_2O$. Hence, combining all factors for the drained treatment, we found hybrid N_2O formation that involves ammonia oxidation as driving process for N_2O emissions (Stieglmeier *et al*., 2014). Another process which might be present under drained conditions could be co-denitrification, but we are not considering it for our study as it is observed under anoxic conditions (Spott *et al*., 2011). Under the flooded treatment, we recorded higher gene copy numbers for *nirK* and *nosZI*. Site preference range (8‰ -20‰) under the anoxic conditions and dominance of denitrifier genes indicate denitrification as the main source process for the small N_2O emissions from the flooded peat (Hu *et al*., 2015). A negative correlation was observed between the abundance of *nosZII* gene in the drained treatment and the abundance of *nosZI* gene in the flooded treatment when compared against N_2O emissions. Espenberg *et al*. (2018) have reported such relations in their study of a tropical fen in French Guiana. This indicates a difference in the ecological niches of *nosZI* and *nosZII* genes (Jones *et al*., 2013; Shan *et al*., 2021). The low emission under flooded conditions could be the result of complete denitrification, leading to a reduction of N_2O to N_2.

CONCLUSIONS

Our study indicates that hybrid N_2O formation that involves ammonia oxidation was the major process of N_2O production in the drained peatland. Denitrification dominated the small emission of N_2O under flooded conditions, possibly due to complete denitrification. Furthermore, we observed that different microbial genes had different niches, which affected the overall microbial processes for N_2O production. *amoA* and *nirS* genes dominated the drained treatment, whereas *nosZ* and *nirK* were more abundant

in the flooded treatment. A combination of isotopic and microbial techniques for partitioning N_2O fluxes yielded additional useful information for N_2O source apportioning. At atomic level, we observed that different tracers ($^{15}NH_4^+$ and $^{15}NO_3^-$) under different treatments (drained and flooded) enriched N_2O molecules with heavy isotopes differently, indicating the presence of separate processes such as hybrid N_2O formation and denitrification.

ACKNOWLEDGEMENT

This study was financially supported by the Ministry of Education and Science of Estonia (No. SF0180127s08), the Estonian Research Council (Nos. IUT2-16, PRG-352, and MOBERC20), the European Union through the European Regional Development Fund (Estonian EcolChange Centre of Excellence, Estonia, and MOBTP101 returning researcher grant by the Mobilitas Pluss programme), and the European Social Fund (Doctoral School of Earth Sciences and Ecology).

SUPPLYMENTARY MATERIAL

Supplementary material for this article can be found in the online version.

CONTRIBUTION OF AUTHORS

MM and ME contributed equally to this work.

REFERENCES

Akima H, Gebhardt A, Petzold T, Maechler M. 2021. Interpolation of irregularly and regularly spaced data. Available online at https://cran.r-project.org/web/packages/akima/ (verified on July 9, 2024)

American Public Health Association-American Water Works Association-Water Environment Federation (APHA-AWWA-WEF). 2005. Standard Methods for the Examination of Water and Wastewater. 21st Edn. APHA-AWWA-WEF, Washington D.C.

Arah J R M. 1992. New formulae for mass spectrometric analysis of nitrous oxide and dinitrogen emissions. *Soil Sci Soc Am J*. **56**: 795–800.

Baggs E M. 2008. A review of stable isotope techniques for N_2O source partitioning in soils: Recent progress, remaining challenges and future considerations. *Rapid Commun Mass Spectrom*. **22**: 1664–1672.

Barnard R, Leadley P W, Hungate B A. 2005. Global change, nitrification, and denitrification: A review. *Glob Biogeochem Cycles*. **19**: GB1007.

Bergsma T T, Ostrom N E, Emmons M, Robertson G P. 2001. Measuring simultaneous fluxes from soil of N_2O and N_2 in the field using the ^{15}N-gas "nonequilibrium" technique. *Environ Sci Technol*. **35**: 4307–4312.

Bol R, Toyoda S, Yamulki S, Hawkins J M B, Cardenas L M, Yoshida N. 2003. Dual isotope and isotopomer ratios of N_2O emitted from a temperate grassland soil after fertiliser application. *Rapid Commun Mass Spectrom*. **17**: 2550–2556.

Buchen C, Lewicka-Szczebak D, Fuß R, Helfrich M, Flessa H, Well R. 2016. Fluxes of N_2 and N_2O and contributing processes in summer after grassland renewal and grassland conversion to maize cropping on a Plaggic Anthrosol and a Histic Gleysol. *Soil Biol Biochem*. **101**: 6–19.

Deppe M, Well R, Giesemann A, Spott O, Flessa H. 2017. Soil N_2O fluxes and related processes in laboratory incubations simulating ammonium fertilizer depots. *Soil Biol Biochem*. **104**: 68–80.

Espenberg M, Truu M, Mander Ü, Kasak K, Nõlvak H, Ligi T, Oopkaup K, Maddison M, Truu J. 2018. Differences in microbial community structure and nitrogen cycling in natural and drained tropical peatland soils. *Sci Rep*. **8**: 4742.

Hallin S, Philippot L, Löffler F E, Sanford R A, Jones C M. 2018. Genomics and ecology of novel N_2O-reducing microorganisms. *Trends Microbiol*. **26**: 43–55.

Hu H W, Chen D L, He J Z. 2015. Microbial regulation of terrestrial nitrous oxide formation: Understanding the biological pathways for prediction of emission rates. *FEMS Microbiol Rev*. **39**: 729–749.

Huang Y, Li Y Y, Yao H Y. 2014. Nitrate enhances N_2O emission more than ammonium in a highly acidic soil. *J Soil Sediment*. **14**: 146–154.

Hyodo A, Malghani S, Zhou Y, Mushinski R M, Toyoda S, Yoshida N, Boutton T W, West J B. 2019. Biochar amendment suppresses N_2O emissions but has no impact on ^{15}N site preference in an anaerobic soil. *Rapid Commun Mass Spectrom*. **33**: 165–175.

Intergovernmental Panel on Climate Change (IPCC). 2021. Climate change 2021: The physical science basis. *In* Masson-Delmotte V, Zhai P, Pirani A, Connors S L, Péan C, Berger S, Caud N, Chen Y, Goldfarb L, Gomis M I, Huang M, Leitzell K, Lonnoy E, Matthews J B R, Maycock T K, Waterfield T, Yelekçi O, Yu R, Zhou B (eds.) Contribution of Working Group I to the Sixth Assessment Report of the Intergovernmental Panel on Climate Change. Cambridge University Press, Cambridge. pp. 3–32.

Jones C M, Graf D R H, Bru D, Philippot L, Hallin S. 2013. The unaccounted yet abundant nitrous oxide-reducing microbial community: A potential nitrous oxide sink. *ISME J*. **7**: 417–426.

Kemmann B, Wöhl L, Fuß R, Schrader S, Well R, Ruf T. 2021. N_2 and N_2O mitigation potential of replacing maize with the perennial biomass crop *Silphium perfoliatum*—An incubation study. *GCB Bioenergy*. **13**: 1649–1665.

Kulkarni M V, Burgin A J, Groffman P M, Yavitt J B. 2014. Direct flux and ^{15}N tracer methods for measuring denitrification in forest soils. *Biogeochemistry*. **117**: 359–373.

Kuypers M M M, Marchant H K, Kartal B. 2018. The microbial nitrogen-cycling network. *Nat Rev Microbiol*. **16**: 263–276.

Levy-Booth D J, Prescott C E, Grayston S J. 2014. Microbial functional genes involved in nitrogen fixation, nitrification and denitrification in forest ecosystems. *Soil Biol Biochem*. **75**: 11–25.

Liu H J, Wrage-Mönnig N, Lennartz B. 2020. Rewetting strategies to reduce nitrous oxide emissions from European peatlands. *Commun Earth Environ*. **1**: 17.

Loftfield N, Flessa H, Augustin J, Beese F. 1997. Automated gas chromatographic system for rapid analysis of the atmospheric trace gases methane, carbon dioxide, and nitrous oxide. *J Environ Qual*. **26**: 560–564.

Ma W K, Bedard-Haughn A, Siciliano S D, Farrell R E. 2008. Relationship between nitrifier and denitrifier community composition and abundance in predicting nitrous oxide emissions from ephemeral wetland soils. *Soil Biol Biochem*. **40**: 1114–1123.

Masta M, Sepp H, Pärn J, Kirsimäe K, Mander Ü. 2020. Natural nitrogen isotope ratios as a potential indicator of N_2O production pathways in a floodplain fen. *Water*. **12**: 409.

McKenney D J, Drury C F, Wang S W. 2001. Effects of oxygen on denitrification inhibition, repression, and derepression in soil columns. *Soil Sci Soc Am J*. **65**: 126–132.

O'Neill R M, Krol D J, Wall D, Lanigan G J, Renou-Wilson F, Richards K G, Jansen-Willems A B, Müller C. 2021. Assessing the impact of long-term soil phosphorus on N-transformation pathways using ^{15}N tracing. *Soil Biol Biochem*. **152**: 108066.

Pärn J, Verhoeven J T A, Butterbach-Bahl K, Dise N B, Ullah S, Aasa A, Egorov S, Espenberg M, Järveoja J, Jauhiainen J, Kasak K, Klemedtsson L, Kull A, Laggoun-Défarge F, Lapshina E D, Lohila A, Lõhmus K, Maddison M, Mitsch W J, Müller C, Niinemets Ü, Osborne B, Pae T, Salm J O, Sgouridis F, Sohar K, Soosaar K, Storey K, Teemusk A, Tenywa M M, Tournebize J, Truu J, Veber G, Villa J A, Zaw S S, Mander Ü. 2018. Nitrogen-rich organic soils under warm well-drained

conditions are global nitrous oxide emission hotspots. *Nat Commun*. **9**: 1135.

Ravishankara A R, Pele A L, Zhou L, Ren Y G, Zogka A, Daële V, Idir M, Brown S S, Romanias M N, Mellouki A. 2019. Atmospheric loss of nitrous oxide (N_2O) is not influenced by its potential reactions with OH and NO_3 radicals. *Phys Chem Chem Phys*. **21**: 24592–24600.

Schmidt H L, Werner R A, Yoshida N, Well R. 2004. Is the isotopic composition of nitrous oxide an indicator for its origin from nitrification or denitrification? A theoretical approach from referred data and microbiological and enzyme kinetic aspects. *Rapid Commun Mass Spectrom*. **18**: 2036–2040.

Sgouridis F, Ullah S. 2015. Relative magnitude and controls of *in situ* N_2 and N_2O fluxes due to denitrification in natural and seminatural terrestrial ecosystems using ^{15}N tracers. *Environ Sci Technol*. **49**: 14110–14119.

Shan J, Sanford R A, Chee-Sanford J, Ooi S K, Löffler F E, Konstantinidis K T, Yang W H. 2021. Beyond denitrification: The role of microbial diversity in controlling nitrous oxide reduction and soil nitrous oxide emissions. *Glob Change Biol*. **27**: 2669–2683.

Smith C J, Nedwell D B, Dong L F, Osborn A M. 2006. Evaluation of quantitative polymerase chain reaction-based approaches for determining gene copy and gene transcript numbers in environmental samples. *Environ Microbiol*. **8**: 804–815.

Smith C J, Osborn A M. 2009. Advantages and limitations of quantitative PCR (Q-PCR)-based approaches in microbial ecology. *FEMS Microbiol Ecol*. **67**: 6–20.

Soosaar K, Mander Ü, Maddison M, Kanal A, Kull A, Lõhmus K, Truu J, Augustin J. 2011. Dynamics of gaseous nitrogen and carbon fluxes in riparian alder forests. *Ecol Eng*. **37**: 40–53.

Spott O, Russow R, Stange C F. 2011. Formation of hybrid N_2O and hybrid N_2 due to codenitrification: First review of a barely considered process of microbially mediated N-nitrosation. *Soil Biol Biochem*. **43**: 1995–2011.

Stevens R J, Laughlin R J. 1998. Measurement of nitrous oxide and dinitrogen emissions from agricultural soils. *Nutr Cycl Agroecosyst*. **52**: 131–139.

Stieglmeier M, Mooshammer M, Kitzler B, Wanek W, Zechmeister-Boltenstern S, Richter A, Schleper C. 2014. Aerobic nitrous oxide production through N-nitrosating hybrid formation in ammonia-oxidizing archaea. *ISME J*. **8**: 1135–1146.

Suenaga T, Ota T, Oba K, Usui K, Sako T, Hori T, Riya S, Hosomi M, Chandran K, Lackner S, Smets B F, Terada A. 2021. Combination of ^{15}N tracer and microbial analyses discloses N_2O sink potential of the anammox community. *Environ Sci Technol*. **55**: 9231–9242.

Sutka R L, Adams G C, Ostrom N E, Ostrom P H. 2008. Isotopologue fractionation during N_2O production by fungal denitrification. *Rapid Commun Mass Spectrom*. **22**: 3989–3996.

Sutka R L, Ostrom N E, Ostrom P H, Breznak J A, Gandhi H, Pitt A J, Li F. 2006. Distinguishing nitrous oxide production from nitrification and denitrification on the basis of isotopomer abundances. *Appl Environ Microbiol*. **72**: 638–644.

Sutka R L, Ostrom N E, Ostrom P H, Gandhi H, Breznak J A. 2003. Nitrogen isotopomer site preference of N_2O produced by *Nitrosomonas europaea* and *Methylococcus capsulatus* Bath. *Rapid Commun Mass Spectrom*. **17**: 738–745.

Toyoda S, Yoshida N. 1999. Determination of nitrogen isotopomers of nitrous oxide on a modified isotope ratio mass spectrometer. *Anal Chem*. **71**: 4711–4718.

Toyoda S, Yoshida N, Miwa T, Matsui Y, Yamagishi H, Tsunogai U, Nojiri Y, Tsurushima N. 2002. Production mechanism and global budget of N_2O inferred from its isotopomers in the western North Pacific. *Geophys Res Lett*. **29**: 1037.

Well R, Flessa H. 2009. Isotopologue signatures of N_2O produced by denitrification in soils. *J Geophys Res Biogeosci*. **114**: G02020.

Well R, Kurganova I, de Gerenyu V L, Flessa H. 2006. Isotopomer signatures of soil-emitted N_2O under different moisture conditions—A microcosm study with arable loess soil. *Soil Biol Biochem*. **38**: 2923–2933.

Xing X Y, Tang Y F, Xu H F, Qin H L, Liu Y, Zhang W Z, Chen A L, Zhu B L. 2021. Warming shapes *nirS*- and *nosZ*-type denitrifier communities and stimulates N_2O emission in acidic paddy soil. *Appl Environ Microbiol*. **87**: e0296520.

Yu L F, Harris E, Lewicka-Szczebak D, Barthel M, Blomberg M R A, Harris S J, Johnson M S, Lehmann M F, Liisberg J, Müller C, Ostrom N E, Six J, Toyoda S, Yoshida N, Mohn J. 2020. What can we learn from N_2O isotope data?—Analytics, processes and modelling. *Rapid Commun Mass Spectrom*. **34**: e8858.

Zaman M, Heng L, Müller C. 2021. Measuring Emission of Agricultural Greenhouse Gases and Developing Mitigation Options using Nuclear and Related Techniques: Applications of Nuclear Techniques for GHGs. Springer, Cham.

Zhu X, Burger M, Doane T A, Horwath W R. 2013. Ammonia oxidation pathways and nitrifier denitrification are significant sources of N_2O and NO under low oxygen availability. *Proc Natl Acad Sci USA*. **110**: 6328–6333.